Multiple RRMs Contribute to RNA Binding Specificity and Affinity for Polypyrimidine Tract Binding Protein†

Ismael Pérez,‡ James G. McAfee,‡ and James G. Patton*

Department of Molecular Biology, Vanderbilt University, Nashville, Tennessee 37235

Received May 19, 1997; Revised Manuscript Received July 15, 1997⊗

ABSTRACT: Polypyrimidine tract binding protein (PTB) is a 57 kD hnRNP protein (hnRNP I) that binds to the pyrimidine tract typically found near the 3′ end of introns. Primary sequence analysis suggests that PTB contains four RNA recognition motifs (RRMs). Data from comparative structural and deletional analysis of PTB are consistent with the presence of a four reiterated domain structure. Since PTB exists in solution as a homodimer, it contains an oligomeric array of eight RRMs. Though the function of RRMs in a monomeric context has been addressed, the significance of their presence in an oligomeric context has not been investigated. To correlate structural motifs with function, we have analyzed the RNA binding properties of wild-type and deletion constructs of PTB that contain RRMs in both an oligomeric and monomeric context. These studies indicate that there is not a strong correlation between the RNA binding affinity and specificity upon oligomerization. However, the mode of RNA interaction and dimerization is linked. We have also found that the primary contributor to the free energy of PTB binding and the primary determinant for RNA binding specificity resides in RRM 3, while the primary contributor to dimer stabilization coincides with residues in RRM 2.

Cellular RNAs are almost always associated with proteins forming ribonucleoprotein particles in both the nucleus and the cytoplasm. A common characteristic of many of the proteins found in these particles is the presence of a relatively conserved domain referred to as the ribonucleoprotein motif (RNP), RNA recognition motif (RRM),[1] or RNA binding domain (RBD; Bandziulis et al., 1989; Kenan et al., 1991; Birney et al., 1993; Burd & Dreyfuss, 1994; Nagai et al., 1995). An RRM is an 80−90 amino acid domain containing two highly conserved internal motifs consisting of conserved octamer (RNP-1) and hexamer (RNP-2) sequences plus additional conserved, mostly hydrophobic, residues throughout the domain. Over 150 members of this family have been identified and their functions vary from nonspecific RNA packaging to specific pre-mRNA splicing regulators (Kenan et al., 1991; Birney et al., 1993; Burd & Dreyfuss, 1994). The solution and/or crystal structure has been determined for individual RRM domains from four different family members (Nagai et al., 1990; Hoffman et al., 1991; Wittekind et al., 1992; Garrett et al., 1994; Lee et al., 1994; Oubridge et al., 1994; Lu & Hall, 1995; Allain et al., 1996). RRMs consist of two α-helices packed against a four-stranded, antiparallel β-sheet. The highly conserved RNP-1 and RNP-2 boxes lie side by side in the two central β-strands, and aromatic residues within these boxes have been proposed to intercalate between the bases of the RNA. The four β-strands provide a platform on which the RNA lies while binding specificity is apparently achieved by amino acid differences in the surrounding variable regions and also by differences in the size and sequence of the loop between β-strands 2 and 3 (Scherly et al., 1990a; Kenan et al., 1991; Nagai et al., 1995).

An interesting feature common to members of this family of RNA binding proteins is that many contain multiple RRMs on a single polypeptide chain. While certain RNA binding proteins apparently require only one RRM to achieve RNA binding specificity and affinity, others have been shown to require combinations of at least two (Lutz-Freyermuth et al., 1990; Nietfeld et al., 1990; Burd et al., 1991; Zamore et al., 1992; Burd & Dreyfuss, 1994; Kanaar et al., 1995; Lu & Hall, 1995; Shamoo et al., 1995). Apparently, contributions from each of the multiple RRMs, or regions outside of these motifs, are needed to achieve wild-type binding specificity and affinity. While it has not been experimentally proven, it appears that individual RRMs within the same protein may allow the binding of multiple RNAs or allow interaction with multiple regions of the same RNA (Lutz-Freyermuth et al., 1990). For example, it has been proposed that the four RRM domains in poly(A) binding protein (PABP) act in pairwise combination to effect interstrand and intrastrand transfer, presumably increasing the efficiency of polyadenylation in

† This work was supported by a grant from the NIH (GM 50418) to J.G.P. I.P. was supported by a MARC Fellowship (GM 17621) and J.G.M. was supported in part by a grant from the Ford Foundation (880-0765). Phosphorimager and fluorescence analyses were made possible by an instrumentation grant from the NSF (BIR-9419667).

* Corresponding author: Department of Molecular Biology, Box 1820 Station B, Vanderbilt University, Nashville, TN 37235. Phone: (615)-322-4738. Fax: (615)-343-6707. Email: PattonJG@Ctrvax.Vanderbilt.edu.

‡ These authors contributed equally to this work.

⊗ Abstract published in *Advance ACS Abstracts,* September 1, 1997.

[1] Abbreviations: CD, circular dichroism; GST, glutathione S-transferase; IPTG, isopropyl β-D-thiogalactopyranoside; hnRNP, heterogeneous nuclear ribonucleoprotein; NLS, nuclear localization signal; PABP, poly(A) binding protein; PTB, (hnRNP I) polypyrimidine tract binding protein; RBD, RNA binding domain; RRM, RNA recognition motif; SSB, single-stranded binding protein.

S0006-2960(97)01174-4 CCC: $14.00

the process (Sachs et al., 1987; Nietfeld et al., 1990; Burd et al., 1991).

RRM domains have also been shown to overlap with nuclear localization signals and with protein−protein interaction domains (Scherly et al., 1990b; Romac et al., 1994; LaCasse & Lefebvre, 1995). However, for many RNA binding proteins, auxiliary domains mediate other functions and can even alter the RNA binding ability of the full-length protein. For example, glycine or glycine-arginine rich domains found in many RRM-containing family members can modulate RNA binding, promote RNA annealing, or mediate protein−protein interaction (Lee et al., 1991; Ghisolfi et al., 1992; Girard et al., 1992; Munroe & Dong, 1992; Casas-Finet et al., 1993; Mayeda et al., 1994; Wang & Bell, 1994). Similarly, a related family of proteins containing regions rich in serine-arginine (SR) dipeptides has been identified in which the SR domains appear to mediate essential protein−protein interactions while the RRM domains mediate RNA binding [reviewed in Fu (1995) and Manley and Tacke (1996)]. Thus, by analogy to transcription factors, RNA binding proteins contain distinct and sometimes separable domains. However, for proteins with multiple RRM domains, the question remains as to why there are multiple domains and what is the function of each domain.

Polypyrimidine tract binding protein (PTB or hnRNP I) is a 57 kD hnRNP protein that binds to the polypyrimidine tract near the 3′ splice site of many introns and can act as a repressor of splicing (Garcia-Blanco et al., 1989; Gil et al., 1991; Patton et al., 1991; Ghetti et al., 1992; Lin & Patton, 1995; Singh et al., 1995; Perez et al., 1997). PTB contains four RRMs but each lacks seemingly critical aromatic amino acids found in conserved positions within consensus RRMs (Kenan et al., 1991; Ghetti et al., 1992; Birney et al., 1993). Such nonconsensus RRMs and other similarities between PTB and hnRNP L have led to the suggestion that these two proteins may represent a new subclass of RRM-containing proteins (Piñol-Roma et al., 1989; Ghetti et al., 1992). In this paper, we show that PTB exists in solution as a dimer, generating a total of eight RRMs potentially involved in RNA binding. To gain insight into the thermodynamic relevance of the oligomeric array of RRMs in PTB, we first identified the regions responsible for stabilizing its dimeric structure, generated deletion constructs of the protein with or without RRMs in oligomeric arrays, and analyzed the equilibrium binding properties of each construct. In contrast to most DNA binding proteins, we have found that RNA binding affinity and specificity are not coupled to oligomerization of PTB. While RRM 3 apparently drives binding specificity and RRM 2 contributes to dimer stabilization, wild-type function is only detected with the intact protein.

MATERIALS AND METHODS

Constructs. GST-PTB, His-PTB, and mutant constructs for recombinant protein expression were made using reverse PCR techniques (Imai et al., 1991; Coolidge & Patton, 1995) to generate deletions or to insert stop codons. The template for all mutant constructs was 121GEX3H [GST-PTB; (Patton et al., 1991)]. For each mutant, the following PTB amino acids were fused to glutathione S-tranferase (GST). Each construct was confirmed by dideoxy nucleotide sequencing (Sequenase).

construct	amino acids
RRM 1	1−131, 526−531
RRM 2	1−16, 170−264, 525−531
RRM 3	323−396
RRM 4	1−16, 437−531
RRM 1-2	1−264
RRM 2-3	1−16, 169−417, 525−531
RRM 3-4	1−16, 323−531
RRM 1-2-3	1−417
RRM 2-3-4	1−16, 170−531
ΔAA1−57 RRM1	58−131, 526−531
AA1−55	1−55

In Vitro Transcription/Translation. In vitro translation reactions for protein−protein interaction studies were performed using the TnT transcription/translation system from Promega. *In vitro* transcription reactions for UV cross-linking studies were performed in 20 μL reactions containing 0.5 mM cap structure [7mG(5′)ppp5′G; NEB], 10 mM DTT, 1× transcription buffer (Promega), 1 unit/μL RNAsin (Promega), 0.5 mM ATP, 0.5 mM UTP, 0.125 mM GTP, 0.125 mM CTP, 20 μCi [^{32}P]CTP, 1 unit/μL SP6 RNA polymerase (Promega), and 1, μg of linearized DNA template.

Protein Purification. BL21 DE3 pLysS containing the appropriate recombinant constructs were grown overnight in 25 mL. of LB media containing 50 μg/mL kanomycin and 25 μg/mL chloramphenicol. Overnights were diluted in 1 L of LB and grown at 37 °C until an OD_{600} of 0.5 was attained. IPTG was then added to a final concentration of 0.4−1 mM, and growth was continued for an additional 2 h at 37 °C for PTB, RRM 1-2-3, and RRM 2-3-4 or 4−5 h for RRM 3-4 and RRM 4. The protein was purified under nondenaturing conditions using Ni-NTA resin (Qiagen). For fluorescence and circular dichroism measurements, the proteins were dialyzed against buffer E (20 mM Tris, pH 8.0, 0.1 mM EDTA) containing the indicated concentration of KCl.

Gel Filtration. A total of 75 μg of recombinant protein in 250 μL of binding buffer (BB) (10 mM Tris-Cl, pH 8.0, 100 mM KCl, 2.5 mM $MgCl_2$, and 5% glycerol) was applied to a Superdex 200 HR10/30 column (Pharmacia) at a flow rate of 0.1 mL/min. Fractions (0.25 mL) were collected and aliquots precipitated with 25% TCA and analyzed on 9% Laemmli gels.

Western Blots. HeLa nuclear extract in 250 μL of BB (50 μL) was fractionated on the same Superdex 200 column as above. Aliquots of each fraction were precipitated, electrophoresed on 9% Laemmli gels, and transferred to PVDF membranes. Visualization was performed using ECL reagents (Amersham) and rabbit anti-human PTB antibodies as described (Patton et al., 1991, 1993). Nuclear extracts were prepared from HeLa cells as described (Patton et al., 1991, 1993).

UV Cross-Linking. UV cross-linking reactions were performed as described (Patton et al., 1991).

Nuclear Localization. Vero cells (monkey kidney cells) were injected with bacterially expressed GST-PTB fusion proteins using an Eppendorf Transjector 5246 mounted on a Zeis IM35 microscope. After injection, cells were incubated for 2 h at 37 °C and 10% CO_2 except for GST-RRM2, which was incubated for 1 h. The cells were then fixed in 4% paraformaldehyde in 1× PBS at room temperature for 20 min, permeabilized with 0.2% Triton-X 100 in 1× PBS at room temperature for 15 min, and washed three

times with PBS. Nonspecific antibody binding sites were blocked by incubating the fixed cells in 10% fetal bovine serum containing 0.2% sodium azide in 1× PBS at room temperature for 1 h. Cells were then incubated with the primary antibody (rabbit α-GST polyclonal) at a 1:100 dilution at room temperature for 2 h. After three 5 min washes in PBS, the secondary antibody (goat α-rabbit Cy3; Jackson ImmunoResearch) was allowed to bind at a 1:400 dilution at room temperature for 1 h. Finally, the cells were washed three times with 1× PBS (5 min each) followed by mounting with 1:10 V/V 1% *p*-phenylenediamine in 1× PBS and glycerol. Staining patterns were visualized using a Zeis Axioplan microscope at 63× magnification.

Fluorescence Measurements. Fluorescence measurements were carried out on an Aminco Bowman AB-2 luminescence spectrometer. Measurements were collected in the ratiometric mode, with excitation and emission slits set at 4 and 8 nM, respectively. Titrations were conducted by exciting a solution of polyethenoadenosine at 310 nm and measuring its emission at 410 nm as a function of increasing protein concentration. Data were fit by nonlinear regression analysis and also by simulation as previously described (McAfee et al., 1995, 1996). Competition titrations, along with the analysis of competiton binding isotherms, were done according to published procedures (McAfee et al., 1996).

Circular Dichroism Measurements. CD spectra were collected at 24 °C on a Jasco 720 spectropolarimeter using a 1 cm path cell. Steady state spectra were derived from an average of 20 different scans recorded at 0.5 nm intervals from 178 to 260 nm. CD spectra were fit using the VARSLC1 computer program supplied by Jasco (Compton & Johnson, 1986; Manavalan & Johnson, 1987).

RESULTS

Domain Organization and Deletion Constructs of PTB. PTB contains four RRMs (Figure 1A) in which the general RRM structure (β-α-β β-α-β) is maintained but apparently crucial aromatic residues found in the β-3 strand (RNP-1 box) and β-1 strand (RNP-2 box) are not conserved with the exception of single aromatic residues in the RNP-1 box of RRMs 1 and 2 (Kenan et al., 1991; Ghetti et al., 1992). No aromatic residues are found in the RNP-2 box in any of the four RRMs. Thus, the RRMs in PTB lack seemingly critical residues, despite a relatively good match to the consensus sequence. On the basis of this conservation, coupled with phylogenetic comparison of PTB between the human, mouse, and *Caenorhabditis elegans* protein sequences, we prepared multiple deletion constructs of PTB for use in studies designed to elucidate the role of individual and multiple RRMs in RNA binding, protein−protein interaction, and nuclear localization (Figure 1).

The First 60 Amino Acids Encode the PTB Nuclear Localization Signal. To map the residues of PTB that direct nuclear localization, GST-PTB fusion proteins were injected into the cytoplasm of Vero cells (monkey kidney cells) followed by indirect immunofluorescence of fixed cells using antibodies against the GST moiety. As shown in Figure 2A, staining of endogenous PTB in Vero cells was consistent with previous localization studies showing that PTB is an abundant nuclear protein with a widespread nucleoplasmic distribution, variably interrupted by discrete perinucleolar spots of high PTB concentration (Ghetti et al., 1992; Matera et al., 1995; Huang et al., 1997) (J. G. Patton and J. Galceran, unpublished results). Injection of full-length PTB fused to GST produced a similar localization of the GST moiety whereas injection of GST protein alone led to cytoplasmic accumulation of GST (Figure 2A). Injection of the deletion constructs shown in Figure 1A showed that a construct containing RRM 1 and the amino terminus of PTB led to import of the fusion protein into the nucleus. All constructs lacking RRM 1 and the amino terminus remained cytoplasmic whereas all constructs retaining this region localized to the nucleus.

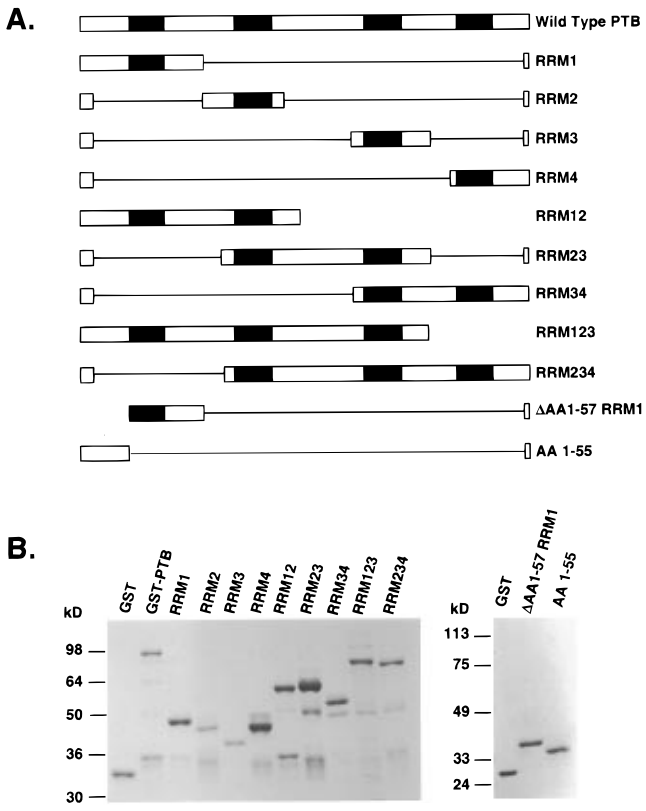

FIGURE 1: Domain structure and deletion clones of PTB. (A) The relative position of the four RRM domains within PTB is shown along with the regions deleted in various constructs. (B) Each of the constructs detailed in Figure 1A were fused to GST and purified by passage over glutathione agarose. An aliquot of each preparation is shown.

To determine whether the nuclear localization signal (NLS) for PTB is present in RRM 1 or the extreme amino terminus (or both), additional GST-PTB fusion constructs were prepared that join either the first 55 amino acids (AA 1−55) or amino acids 57−131 (ΔAA 1−57 RRM 1) of PTB to GST. As shown in Figure 2B, deletion of the amino terminus from the RRM 1 construct resulted in mostly cytoplasmic localization with only slight nuclear accumulation. In contrast, fusion of amino acids 1−55 to GST led to complete nuclear import of the GST moiety showing that the NLS for PTB is located within this domain.

PTB Is Structurally Symmetrical around RRMs 2 and 3. Once the nuclear localization signal was found to utilize residues distinct from any of the four putative RRMs, it was of interest to determine how each of these RRMs contribute to the structure and function of PTB. Therefore, we used circular dichroism spectroscopy to analyze the secondary structural content of recombinant, histidine-tagged PTB and a selected subset of histidine-tagged deletions of the wild-

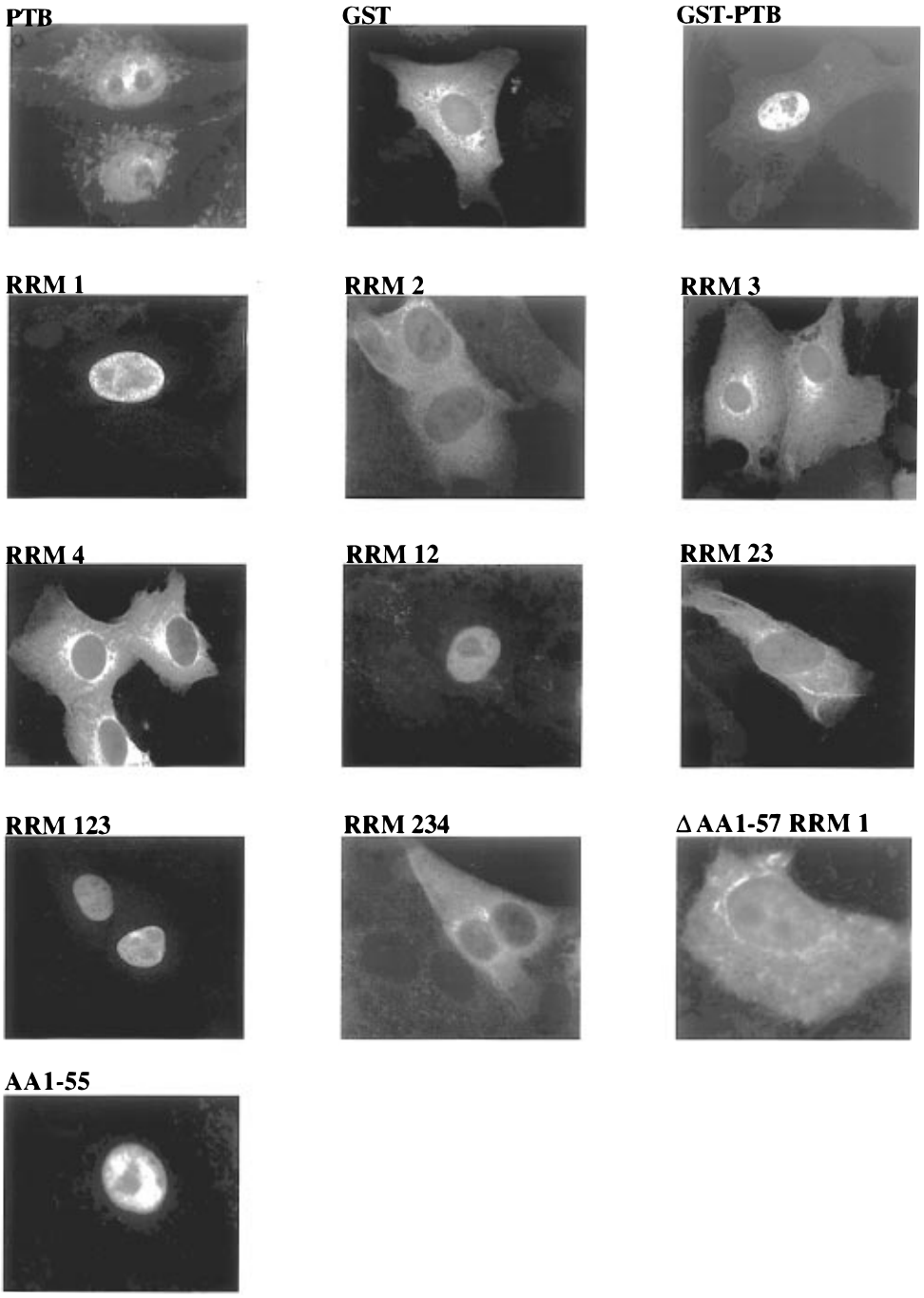

FIGURE 2: The amino terminus of PTB encodes the nuclear localization signal. Monkey kidney cells (Vero cells) were injected with the indicated GST fusion proteins followed by immunolocalization of the GST moiety. The localization of endogenous PTB is shown at the top left using polyclonal antibodies against human PTB. The region of PTB included in each deletion construct is as indicated in Figure 1A. It should be stressed that the RRM 1 construct contains both the amino terminus of PTB (amino acids 1−55) in addition to RRM 1.

type protein (RRM 1-2-3, RRM 2-3-4, and RRM 3-4; see Figure 1A) to gain empirical evidence that the protein consists of a four domain structure. We reasoned that the structural composition of a polypeptide generated by cleavage between RRMs 2 and 3 would be the same as an asymmetric deletion of the amino terminal RRM (RRM 1) or the carboxy terminal RRM (RRM 4). Furthermore, each of these deletion constructs should have the same percentage of secondary structural elements as the wild-type protein. All four constructs showed significant negative ellipticity in the region between 208 and 222 nm, indicating that the proteins retain structure and, as predicted for a four RRM domain protein, the CD spectra for all four proteins were nearly identical (data not shown). This is quantitatively presented in Table 1, where fits of all four CD spectra indicate essentially identical percentages of α-helices, β-sheets, β-turns, and

Table 1. Percentage of Structural Elements Determined by Variable Selection Analysis of CD Spectra[a]

domain	helix	β-sheet (A)	β-sheet (P)	turns	other	total
RRM 1-2-3	26(1)	10(1)	0(0)	22(1)	42(1)	100
RRM 2-3-4	27(1)	11(2)	1(0)	21(1)	44(1)	103
RRM 3-4	25(1)	13(1)	1(0)	18(0)	43(1)	101
PTB	25(1)	12(3)	1(1)	19(2)	44(2)	101

[a] Shown are the percentages of α-helices, β-sheets (A = antiparallel and P = parallel), turns, and other secondary structural elements. The values in parentheses represent the standard deviations calculated from the fits.

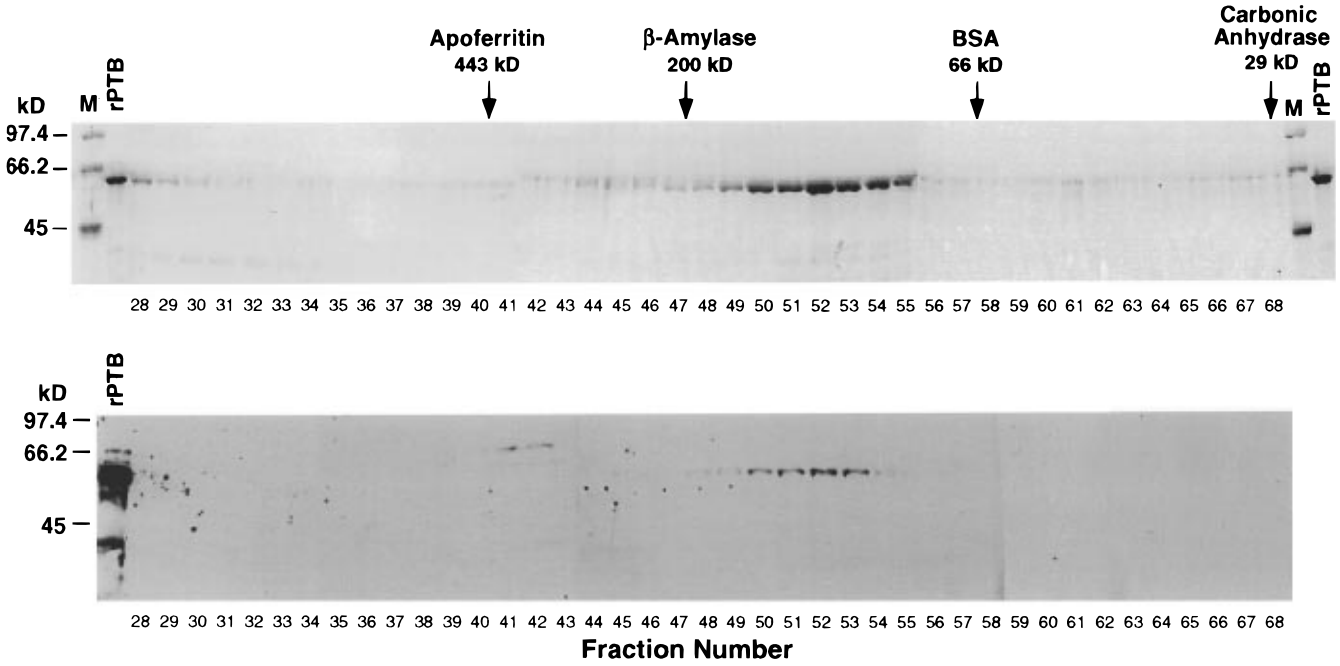

FIGURE 3: Gel filtration analysis of PTB. Recombinant PTB (rPTB; top) was applied to a Superdex 200 gel filtration column and aliquots of various fractions were precipitated and analyzed by SDS−PAGE. The starting material is shown adjacent to SDS molecular weight marker lanes (M) and the elution pattern of four chromatography marker proteins and their sizes are as indicated. In the lower panel, HeLa nuclear extract was fractionated on the same Superdex 200 column and fractions were again precipitated and separated by SDS−PAGE. Proteins were transferred to PVDF membranes, and Western blots were performed to visualize PTB using anti-PTB antibodies. A lane of control protein (antigen) is shown at the left.

other structures. These data confirm the consensus analysis and indicate that PTB has a reiterated four domain structure that is symmetrical around RRMs 2 and 3. Furthermore, the CD spectra show that there is no major domain disruption generated in the PTB deletion constructs.

Oligomerization Determinants of PTB. To examine the oligomeric state of PTB, recombinant PTB and HeLa nuclear extracts were subjected to size exclusion chromatography under nondenaturing conditions. This analysis showed that, under these conditions, rPTB eluted with an apparent molecular mass of 114 kDa which corresponds to the expected mass of a dimer (Figure 3). Furthermore, fractionation of HeLa nuclear extract followed by Western blot analysis showed that the majority of PTB present in nuclear extract also eluted with a molecular mass corresponding to that of a dimer (Figure 3). In addition, the yeast two-hybrid assay was used to show that PTB interacts with itself approximately 300-fold stronger than with a variety of negative control partners (data not shown). Thus, PTB exists in solution as a dimer, combining a total of eight RRM domains within one complex, raising the question as to the individual contribution of each of these putative domains to the overall function of PTB.

PTB−PTB Interaction Domains. To identify the domains necessary for PTB−PTB interaction, wild-type PTB was *in vitro* translated and the ^{35}S-labeled protein was incubated with relatively equal amounts of the various resin-bound GST-PTB mutant proteins. After a short incubation period, the complexes were washed several times after which the resin-bound proteins were eluted and analyzed by SDS−PAGE (Figure 4). Any GST-PTB deletion construct capable of interacting with wild-type PTB should cause retention of ^{35}S-labeled, full-length PTB. Figure 4 shows that constructs containing RRMs 1-2, 2-3, 1-2-3, and 2-3-4 caused retention of wild-type PTB. None of the single RRMs, nor a combination of RRMs 3-4, were capable of interaction. As expected, full length GST-PTB interacted with ^{35}S-labeled PTB. By examining the amino acids present in each of these constructs (see Materials and Methods and Figure 1A), residues that apparently stabilize dimer formation can be mapped to amino acids 169−264. Since RRM 2 is incapable of supporting interaction, additional residues outside of this region must contribute to the overall free energy of dimer formation.

To confirm the validity of the *in vitro* interaction assay, we analyzed the oligomerization state of the RRM 1-2-3 and RRM 2-3-4 constructs by size exclusion chromatography. Although approximately 90% or more of both of these two species eluted with a mass corresponding to that of a monomer, protein could be detected in the dimer region of the elution profile (data not shown). Size exclusion analysis of the RRM 3-4 construct demonstrated that this species was strictly a monomer in solution. These findings further suggest that residues within RRM 2 probably contribute the most to the free energy of dimer formation, while residues outside of this region are necessary to completely stabilize the oligomeric state.

Primary Determinants of PTB That Govern RNA Binding Affinity and Specificity. Since UV-cross-linking studies are insightful with regard to exploring the interaction geometry of protein−nucleic acid complexes, we used this assay to gain initial information as to which of the four potential RRMs might play a role in RNA binding specificity. In these studies, proteins were incubated with a ^{32}P-labeled RNA probe and subjected to UV cross-linking. We used an RNA probe consisting of the branchpoint/polypyrimidine tract (B3P3) upstream of α-tropomyosin exon 3 (B3P3) since PTB has been shown to bind specifically to this RNA (Mullen et al., 1991; Patton et al., 1991). As before, full-length PTB, either in HeLa nuclear extract or fused to GST, efficiently

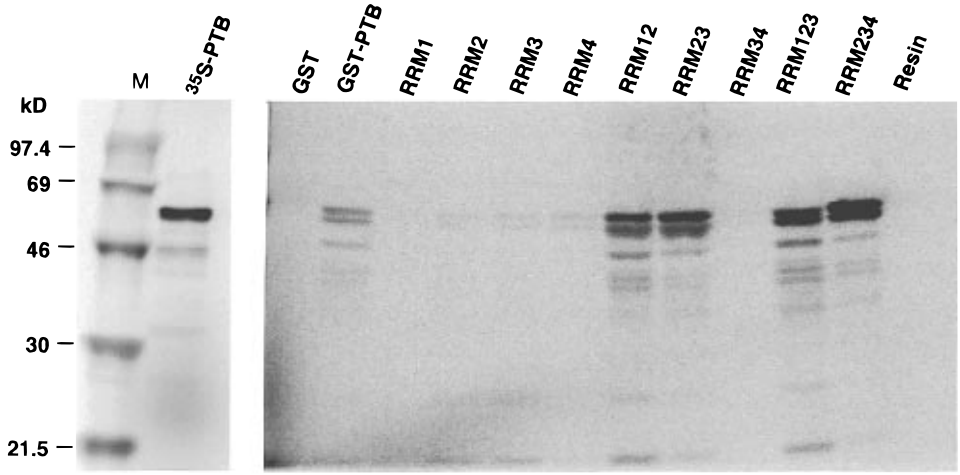

FIGURE 4: RRM 2 and oligomerization of PTB. GST-PTB fusion proteins were purified as shown in Figure 1A and incubated with *in vitro* translated, ^{35}S-labeled PTB (left panel). The resulting complexes were captured by passage over glutathione agarose and bound proteins were eluted and analyzed by SDS−PAGE and autoradiography.

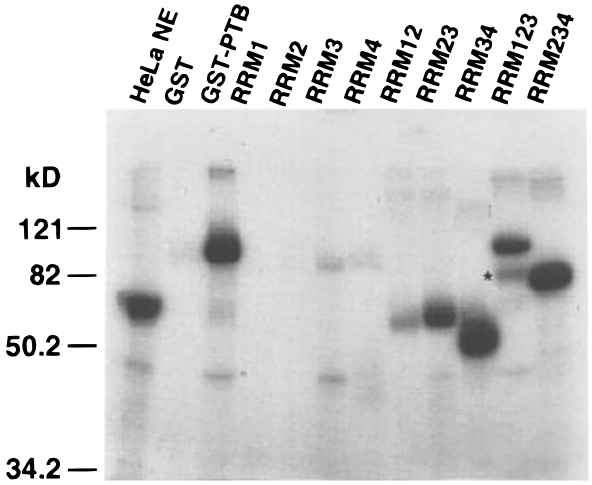

FIGURE 5: RNA binding specificity and RRMs 3-4. Protein constructs as depicted in Figure 1A were incubated with a ^{32}P-labeled polypyrimidine tract containing RNA and subjected to UV light. Following digestion with RNAse A, ^{32}P-labeled proteins were separated by SDS−PAGE. A control cross-linking reaction was performed by incubation of the RNA probe with HeLa nuclear extract (NE) resulting in the labeling of PTB. The remaining proteins are as indicated. Marker protein sizes are depicted at the left. The asterisk indicates the major RRM 1-2-3 protein whereas the cross-linked band in this lane is due to read-through translation generating a minor amount of full−length PTB which is efficiently cross-linked.

cross-linked to the B3P3 probe (Figure 5). In addition, PTB constructs containing RRMs 2-3, 3-4, and 2-3-4 also efficiently cross-linked to the B3P3 RNA. None of the constructs containing single RRMs were capable of efficient cross-linking while constructs containing RRMs 1-2 and 1-2-3 cross-linked to B3P3 RNA but very inefficiently as compared to the RRM 3-4 or 2-3-4 constructs. The major cross-linked product in the RRM 1-2-3 preparation is due to minor contaminating amounts of wild-type GST-PTB (produced by read-through translation) and not to the predominant RRM 1-2-3 protein (compare Figure 1A with Figure 5). The RRM 3-4 construct was the most efficiently cross-linked protein suggesting that this species contains the minimal primary sequence responsible for specific RNA interactions.

Equilibrium RNA Binding Studies. Our results and previous studies confirm that PTB binds specifically to pyrimidine-rich sequences. However, these observations were derived from nonequilibrium analyses (Garcia-Blanco et al., 1989; Mullen et al., 1991; Patton et al., 1991). UV-cross-linking is instrumental in exploring complex geometry but it does not quantitatively address RNA binding affinity and other characteristic thermodynamic parameters associated with protein−nucleic acid interactions (i.e., occluded binding site size, cooperativity, etc) Thus, to more quantitatively explore the RNA binding properties of PTB, we used fluorescence spectroscopy to evaluate equilibrium binding parameters for the interaction of PTB with the fluorescently labeled RNA substrate, polyethenoadenosine (poly[ϵ(A)]). Furthermore, we determined equilibrium binding parameters for the interaction of PTB with poly(A), poly(C), poly(G), and poly(U) RNA by analyzing the effect of these nucleic acids on the fractional saturation of the fluorescent substrate in competition titrations (McAfee et al., 1996). Shown in Figure 6A is a binding isotherm for the interaction of PTB with poly[ϵ(A)] and competition isotherms for the interaction of the protein with poly(C), (U), (G), and (A) RNA (Figure 6, panels B−E, respectively). The data shown in Figure 6 were analyzed by simulating theoretical sets of data to fit the experimental data (McGhee von-Hippel, 1973; McAfee et al., 1996) or by nonlinear regression analysis using the McGhee von Hippel noncooperative model (McAfee et al., 1995). In general, simulated fits were comparable to those obtained by nonlinear least-squares analysis. From the analysis shown in Figure 6A, PTB was found to bind poly-[ϵ(A)] with an intrinsic association constant (K_i) of 4.9×10^6 M^{-1} and an occluded binding site size (n) of 33 nucleotides/dimer. An analysis of the binding isotherms in panels B−D of Figure 6 shows that the protein exhibits a marked preference for binding polypyrimidines, as previously reported. The K_i determined for the interaction of PTB with poly(C) and poly(U) RNA was comparable (8×10^7 and 2×10^8 M^{-1} for poly(C) and poly(U), respectively) while that for its interaction with poly(G) RNA was somewhat lower (1×10^{-7} M^{-1}). An inability to observe inhibition of the poly[ϵ(A)] fluorescence enhancement in the presence of a 2-fold M excess of poly(A) suggests that the affinity of PTB for poly(A) RNA is much, much less than that of poly[ϵ-(A)].

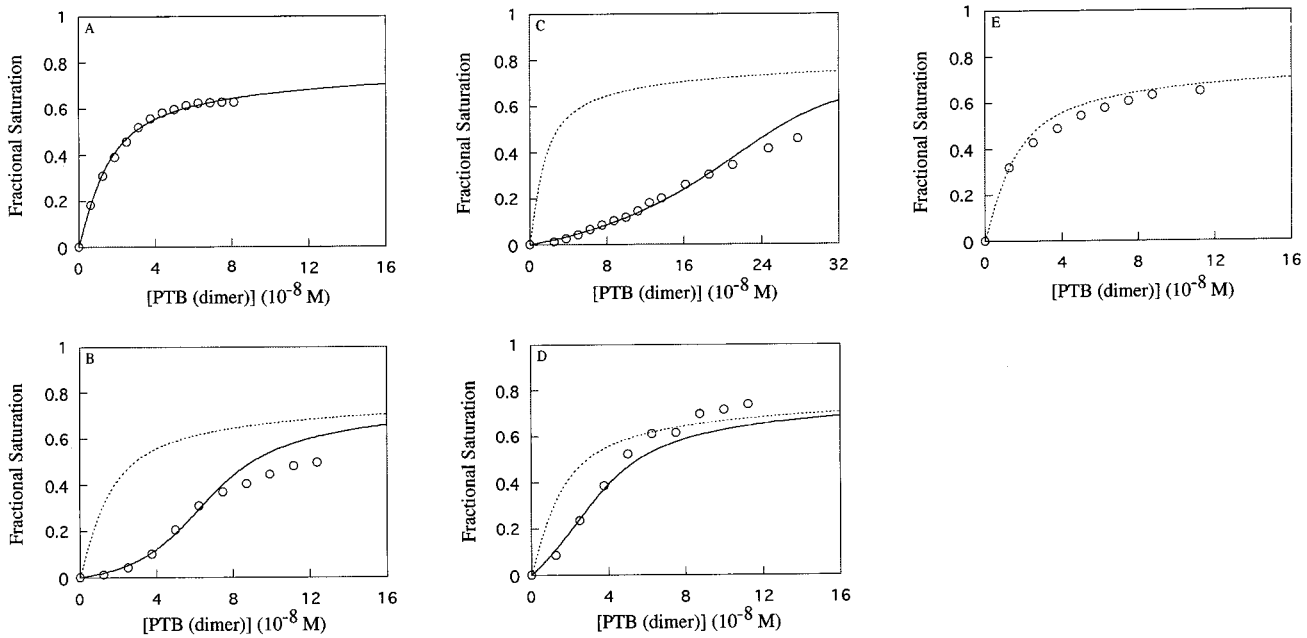

FIGURE 6: Equilibrium binding analysis of PTB. Shown are binding isotherms for the interaction of PTB with 0.8 mM of poly[ϵ(A)] alone (panel A) or with 0.8 mM of poly[ϵ(A)] and a 2-fold molar excess of one of the following competitors; poly(C) (panel B), poly(U) (panel C), poly(G) (panel D), and poly(A) (panel E). All titrations were conducted in buffer E containing 100 mM KCl. The solid line in each panel represents fits of the experimental data (circles) to the McGhee von Hippel noncooperative binding model. For titrations conducted in the presence of a competitor nucleic acid (panels B−E), the dashed line is the same as the solid line in panel A and is the fitted curve for the interaction of PTB with poly[ϵ(A)] in the absence of competitor. The intrinsic association constants, K_i, for the interaction of PTB with poly[ϵ(A)], poly(C), poly(U), and poly(G) were 4.9×10^6, 8×10^7, 2×10^8, and 1×10^7 M^{-1}, respectively. The corresponding site sizes evaluated from the fits were $n = 33$, 18, 5, and 33 for the interaction of PTB with poly[ϵ(A)], poly(C), poly(U), and poly(G), respectively. At a 2-fold molar excess of poly(A) inhibition of the poly[ϵ(A)] fluorescence enhancement could not be observed indicating that the affinity of PTB for this substrate is much less than that observed for the interaction of the protein with poly[ϵ(A)], accounting for the lack of a solid line in Figure 6E.

Having determined thermodynamic parameters for the interaction of PTB with poly[ϵ(A)] and poly(U), these two substrates were then used to quantitatively probe determinants in PTB that govern RNA binding affinity and specificity. First, equilibrium constants were determined for the interaction of RRM 1-2-3, RRM 2-3-4, and RRM 3-4 with poly[ϵ(A)] in buffer containing 100 mM KCl. From Figure 7A, the affinity constants (K_i) for the interaction of RRM 1-2-3, RRM 2-3-4, and RRM 3-4 with the fluorescent substrate were 3×10^5, 5×10^5, and 5×10^7 M^{-1}, respectively. Thus, monomeric deletion constructs of PTB lacking one (RRM 2-3-4) or two (RRM 3-4) amino or carboxy terminal (RRM 1-2-3) RRMs retain RNA binding activity, albeit with less affinity. It is interesting to note that in addition to the lower poly[ϵ(A)] binding affinity observed for the deletion constructs, the molecular mode of the interaction (defined by the occluded site size and the difference in the maximum observed enhancement) was found to be different than that of full-length PTB. The occluded binding site size observed for the wild-type protein was ~16 nucleotides/monomer, while the sizes observed for RRM 1-2-3, RRM 2-3-4, and RRM 3-4 were 30, 81, and 26 nucleotides/monomer, respectively. Although these data suggest that deletion of the protein has generated an alternative interaction with the fluorescent substrate, the competition binding studies shown in Figure 7, panels B and C, demonstrate that the sequence-specific binding characteristics of each mutant construct are preserved. Because the fractional change in the fluorescence enhancement was low in the range of protein concentration used at 100 mM KCl, these experiments were also performed at lower ionic strength (70 mM KCl). Like the wild-type protein, RRM 1-2-3 and RRM 2-3-4 both bound poly(U) RNA with an affinity exceeding that of the nonspecific substrate (poly [ϵ-(A)]) by more than 10-fold. No sequence-specific recognition was observed for the interaction of any of our constructs with poly(A) RNA (data not shown). Because RRM 3-4 exhibited very little protein-induced poly[ϵ(A)] enhancement at 100 mM KCl, a competition titration was conducted in buffer at 40 mM KCl. As shown in Figure 7D, sequence-specific recognition of poly(U) RNA is still maintained by this construct, consistent with the UV-cross-linking experiments.

DISCUSSION

Function of Multiple RRMs. A common feature of many RNA binding proteins is the presence of multiple RNA binding domains both in the RRM family as well as in the family of double-stranded RNA binding proteins and RNA binding proteins containing RGG repeats and KH domains (Kiledjian & Dreyfuss, 1992; Birney et al., 1993; Burd & Dreyfuss, 1994; Kharrat et al., 1995; Musco et al., 1996). While many proteins, both RNA binding proteins and otherwise, contain defined modular domains that can function independently or in combination with unrelated domains from other proteins, the presence and function of multiple RRM domains remains a common but poorly understood phenomenon. We have mechanistically addressed several significant facets with regard to the oligomeric array of RRMs in PTB and how they function in RNA recognition. First of all, we find that the entire protein is required for wild-type RNA binding specificity and affinity, though the major contributor to these actions is apparently derived from RRM 3. Secondly, we find that, unlike many DNA binding proteins,

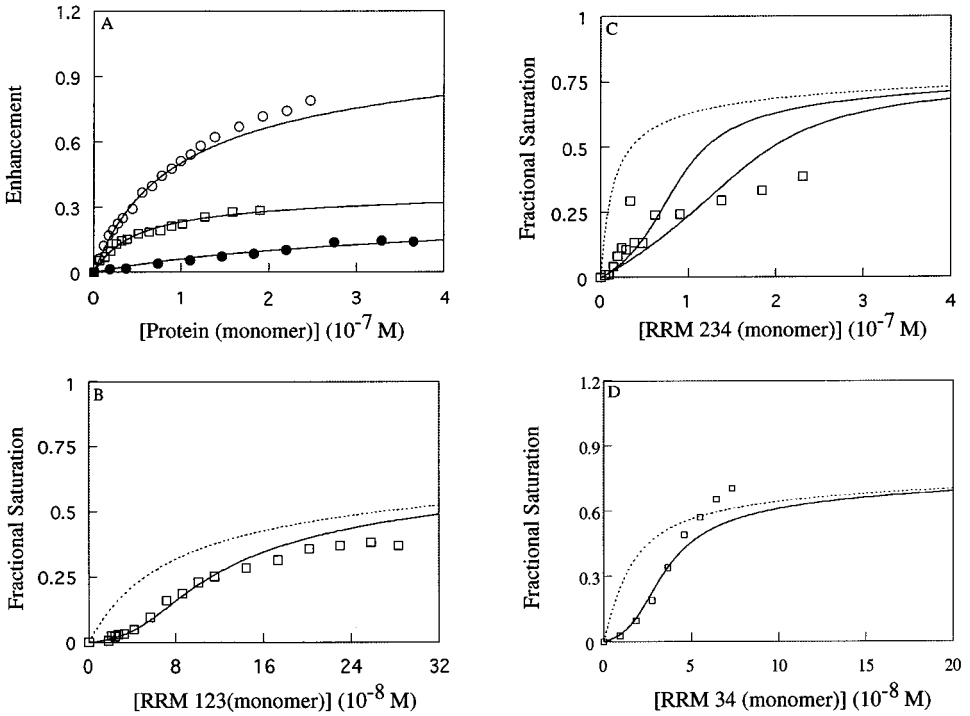

FIGURE 7: Equilibrium binding analysis of RRMs 1-2-3, 2-3-4, and 3-4. Shown in panel A are binding isotherms for the interaction of RRM 1-2-3 (open circles), RRM 2-3-4 (squares), and RRM 3-4 (filled circles) with 1 mM of poly[ϵ(A)] in buffer D containing 100 mM KCl. The data were fit to the McGhee von Hippel noncooperative binding model assuming a K_i of 3.0×10^5, 5×10^5, and 7×10^4 M^{-1} for the interaction of RRM 1-2-3, RRM 2-3-4, and RRM 3-4 with poly[ϵ(A)], respectively. The binding site sizes determined for interaction of these same constructs were 30, 81, and 26 nucleotides for RRM 1-2-3, RRM 2-3-4, and RRM 3-4. Panels B−D are data from competition binding experiments conducted with 1 mM of poly[ϵ(A)] and 1 μM poly(U) with either RRM 1-2-3 (panel B), RRM 2-3-4 (panel C), or RRM 3-4 (panel D). These titrations were conducted in buffer E containing 70 mM KCl (panels B and C) or 40 mM KCl (D). The data were fit using the McGhee von Hippel noncooperative equation assuming K_i and an n of 2×10^7 M^{-1} and 11 nucleotides (RRM 1-2-3) and 5×10^7 M^{-1} and 8 nucleotides (RRM 3-4). The competition data for RRM 2-3-4 could not be used to reveal reliable parameters. However, shown in panel C are two simulated curves assuming a K_i of 5×10^7 M^{-1} and an n of 4 nucleotides (left curve) or a K_i of 5×10^7 M^{-1} and an n of 8 nucleotides. The level of poly[ϵ(A)] inhibition observed in this experiment is consistent with a K_i above 10^7, indicating that the uncertainty in the fit lies in the estimation of n.

RNA binding affinity and specificity are not synergistically coupled to oligomerization of PTB. Our approach to addressing some of these issues may shed light on previous nonequilibrium approaches that sought to correlate RRM structural motifs with function. For example, in the analysis of the function of the four RRMs in poly(A) binding protein, it was suggested that pairwise combination of any of the four (I/II, II/III, and III/IV) RRMs were required for RNA binding (Burd et al., 1991). These studies did not take into consideration that the lack of activity observed for some of their deletions might have resulted from domain disruption. Thus, the pairwise combination of RRMs required for binding RNA in their assay may have actually resulted from an inability to separate the contiguous RRMs without domain disruption, or possibly, disruption of the quaternary structure of the protein. In our approach, we have taken care to demonstrate by spectroscopic analysis that PTB does indeed contain a four domain structure and that the deletion constructs used in our equilibrium binding analyses maintain structure.

We have also evaluated the state of oligomerization of PTB and have determined the effect of this parameter on RNA binding affinity and specificity. Although the function of multiple RRMs within a monomer context has been previously investigated, their function in an oligomeric array has not been studied. In fact, several studies which have investigated the function of multiple RRMs failed to evaluate the oligomeric state of the protein under study. In many multimeric DNA binding proteins, it has been shown that DNA binding affinity is coupled to oligomerization. Therefore, when mapping domain function using deletional analysis, not only must the primary sequence be taken into consideration, but also the oligomeric state of the resulting construct. This oversight can essentially convert a potentially multidimensional problem to a single dimension, and grossly oversimplify data analysis. For example, in many cases involving oligomeric DNA binding proteins, increasing the subunit composition of the protein increases the surface area contacts that the protein can generate with the nucleic acid thereby synergistically influencing affinity. Multiple subunits may also allow the protein to interact with the nucleic acid in more than one state or binding mode. SSB from *Escherichia coli* exists in solution as a homotetramer, and it has been demonstrated that DNA binding can occur with two (SSB_{35} complex) or four (SSB_{65} complex) subunits bound (Griffith et al., 1984; Lohman & Overman, 1985; Bujalowski & Lohman, 1986). The number of interacting subunits is ionic strength dependent, and two subunits bound to single-stranded DNA is characterized by a different set of thermodynamic interaction parameters than with four subunits interacting (Lohman & Bujalowski, 1990). Thus, the presentation of a nucleic acid binding surface in an oligomeric context can generate more than one type of bound complex which may be regulated *in vitro* or *in vivo* by solution conditions. Complex diversity can therefore render a protein multifunctional which may explain a role for SSB

in DNA replication, recombination, and repair (Williams et al., 1984; Lohman et al., 1988).

Similar to SSB, a number of functions have been reported for PTB including regulation of cap-independent translation of picornavirus mRNAs, regulation of 3′ splice site selection, pre-mRNA packaging, and even transcriptional activation (Jansen-Durr et al., 1992; Dreyfuss et al., 1993; Jackson & Kaminski, 1995; Lin & Patton, 1995; Singh et al., 1995; Perez et al., 1997). It seems probable that the oligomeric state of PTB, like SSB, could allow for the formation of a number of different complexes altering its mode of interaction with distinct RNAs promoting diverse functional activities. This is supported by our equilibrium binding experiments that indicated that PTB can form thermodynamically distinct, RNA sequence-dependent complexes accounting for the different site sizes and association constants observed for the interaction of PTB with poly(U), poly(C), poly(G), and poly[ϵ(A)].

Nuclear Localization Signal for PTB. We have found that the PTB NLS resides within the first 55 amino acids, consistent with recent experiments that showed that a region including the amino terminus contains the NLS (Huang et al., 1997). Comparison of the amino acids within this domain (amino acids 1−55) suggests that the PTB NLS does not match the SV40 NLS and instead appears to resemble a bipartite NLS with the exception that the distance between the two elements (29 amino acids) is somewhat larger than the normal 10 amino acids (Dingwall & Laskey, 1991; Gorlich & Mattaj, 1996). Nevertheless, the amino acids in each half of the bipartite signal closely match the normal bipartite consensus signals (derived from nucleoplasmin; see below). Both halves of this sequence are apparently required as many of the injected constructs contain the first 16 amino acids (see Materials and Methods) yet fail to localize to the nucleus. As expected, the NLS sequence is conserved but the distance between the bipartite signals (indicated by dashes) appears variable.

C. elegans PTB	GR**KR**G----------**KKAK**
mouse PTB	GT**KR**G----------**KKFK**
human PTB	GT**KR**G----------**KKFK**
dog PTB	GT**KR**G----------**KKFK**
nucleoplasmin	AV**KR**P----------**KKKK**

RRM 2 and Oligomerization of PTB. Our analyses suggest that, under the conditions used in our experiments, PTB contains four reiterated domains and exists in solution as a dimer. Deletion of either the amino (RRM 2-3-4 construct), or carboxy terminal RRMs (RRM 1-2-3 construct) generated species where the direction of equilibrium is shifted toward the monomer state. Deletion of RRMs 1 and 2 (RRM 3-4 construct) shifted equilibrium completely in the direction of the monomer. The incubation of ^{35}S-labeled PTB with equal amounts of GST-PTB mutant proteins showed that RRMs 1−2, 2−3, 1-2-3, and 2-3-4 were able to interact with wild-type PTB while none of the single RRMs nor a combination of RRMs 3-4 were capable of interaction. These data suggest that RRM 2 is minimally required to maintain homotypical protein−protein interaction, while determinants outside of this region are apparently required to further stabilize the dimer state.

Oligomerization of PTB, RNA Binding and Specificity. The UV-cross-linking data in Figure 5 suggest that RRM 3-4 might represent the minimal RNA specificity domain. In addition, the efficiency of cross-linking for this construct and RRM 2-3-4, which are both monomers, was comparable to that observed for the wild-type PTB dimer, implying that RNA binding specificity is not linked to oligomerization. However, because cross-linking efficiency does not necessarily correlate with affinity, we used fluorescence spectroscopy to determine steady state binding parameters for the interaction of wild-type PTB and the monomeric deletion constructs, RRM 1-2-3, 2-3-4, 3-4, and 4 to various homoribopolymers. These constructs all exhibited RNA binding activity, but the mode of interaction of these species with poly[ϵ(A)] was distinctly different from that of the wild-type protein. Surprisingly, all three constructs maintained the poly(U) binding specificity of full-length PTB, indicating that sufficient primary sequence was available to maintain RNA binding specificity and that dimer formation was not required for RNA binding specificity. In addition, there was not a large difference in the free energy of the binding reaction between the dimeric wild-type protein and the monomeric deletion constructs RRM 1-2-3 and RRM 2-3-4. The calculated change in free energy for the binding of PTB, RRM 1-2-3, RRM 2-3-4, and RRM 3-4 to poly[ϵ(A)] was −361, −308, −321, and −272 kcal/mol, respectively. Thus, neither RNA binding specificity nor affinity is directly linked to oligomerization.

RNA Binding Specificity and RRM 3. From the analysis of the binding behavior of the three deletion constructs, RRM 1-2-3, RRM 2-3-4, and RRM 3-4, it can be deduced that RRM 3 represents the minimal domain required for sequence specific RNA recognition. Since the free energies of complexation for RRM 1-2-3 and 2-3-4 with both poly[ϵ-(A)] and poly(U) were comparable, the contributions of RRM 1 and 4 are minimal with regard to the total free energy of the binding reaction. The high efficiency of cross-linking of RRM 3-4 to the B3P3 RNA, the lack of a significant difference in free energy between the wild-type PTB−poly-[ϵ(A)] and RRM 3-4−poly[ϵ(A)] complex, and the insignificant contributions from RRMs 1 and 4 all confirm that RRM 3 is the major determinant for RNA binding affinity and specificity. However, residues outside of RRM 3 are also needed for sequence specific recognition since it appears that electrostatic interactions play a more important role in the binding of RRM 3-4 to poly[ϵ(A)] than the binding of PTB, RRM 1-2-3, or RRM 2-3-4 to poly[ϵ(A)]. Thus, RRM 3 may be sufficient to generate RNA binding specificity, but overall complex stabilization requires additional residues that render such complexes resistant to dissociation at elevated ionic strength. These additional residues apparently reside within the other RRMs consistent with the fact that wild-type affinity and specificity for PTB requires contributions from all of the RRMs. This may provide a mechanistic explanation for the observation that multiple deletions of PTB failed to mimic wild-type activity even though RNA binding properties were preserved (Kaminski et al., 1995; Huang et al., 1997).

ACKNOWLEDGMENT

Special thanks to Drs. Ellen Fanning and Achim Dickmanns for help with the microinjections and to Dr. Wallace LeStourgeon for critical evaluation of the manuscript.

SUPPORTING INFORMATION AVAILABLE

Figures of CD spectra of wild-type and deletion constructs of PTB and primary sequence analysis of PTB (5 pages). Ordering information is given on any current masthead page.

REFERENCES

Allain, F. H.-T., Gubser, C. C., Howe, P. W. A., Nagai, K., Neuhaus, D., & Varani, G. (1996) *Nature 380*, 646−650.

Bandziulis, R. J., Swanson, M. S., & Dreyfuss, G. (1989) *Genes Dev. 3*, 431−437.

Birney, E., Kumar, S., & Krainer, A. R. (1993) *Nucleic Acids Res. 21*, 5803−5816.

Bujalowski, W., & Lohman, T. M. (1986) *Biochemistry 25*, 7799−7802.

Burd, C. G., & Dreyfuss, G. (1994) *Science 265*, 615−621.

Burd, C. G., Matunis, E. L., & Dreyfuss, G. (1991) *Mol. Cell. Biol. 11*, 3419−3424.

Casas-Finet, J. R., Smith, J. D., Kumar, A., Kim, J. G., Wilson, S. H., & Karpel, R. L. (1993) *J. Mol. Biol. 229*, 873−889.

Compton, L. A., & Johnson, W. C. (1986) *Anal. Biochem. 155*, 155−167.

Coolidge, C. J., & Patton, J. G. (1995) *Biotechniques 18*, 763−764.

Dingwall, C., & Laskey, R. A. (1991) *Trends Biochem. Sci. 16*, 478−481.

Dreyfuss, G., Matunis, M. J., Piñol-Roma, S., & Burd, C. G. (1993) *Annu. Rev. Biochem. 62*, 289−322.

Fu, X.-D. (1995) *RNA 1*, 663−680.

Garcia-Blanco, M. A., Jamison, S. F., & Sharp, P. A. (1989) *Genes Dev. 3*, 1874−1886.

Garrett, D. S., Lodi, P. J., Shamoo, Y., Williams, K. R., Clore, G. M., & Gronenborn, A. M. (1994) *Biochemistry 33*, 2852−2858.

Ghetti, A., Piñol-Roma, S., Michael, W. M., Morandi, C., & Dreyfuss, G. (1992) *Nucleic Acids Res. 20*, 3671−3678.

Ghisolfi, L., Kharratt, A., Joseph, G., Amalric, F., & Erard, M. (1992) *Eur. J. Biochem. 209*, 541−548.

Gil, A., Sharp, P. A., Jamison, S. F., & Garcia-Blanco, M. A. (1991) *Genes Dev. 5*, 1224−1236.

Girard, J.-P., Lehtonen, H., Caizergues-Ferrer, M., Amalric, F., Tollervey, D., & Lapeyre, B. (1992) *EMBO J. 11*, 673−682.

Görlich, D., & Mattaj, I. W. (1996) *Science 271*, 1513−1518.

Griffith, J. D., Harris, L. D., & Register, J. (1984) *Cold Spring Harbor Symp. Quant. Biol. 49*, 553−559.

Hoffman, D. W., Query, C. C., Golden, B. L., White, S. W., & Keene, J. D. (1991) *Proc. Natl. Acad. Sci. 88*, 2495−2499.

Huang, S., Deerinck, T. J., Ellisman, M. H., & Spector, D. L. (1997) *J. Cell Biol. 137*, 956−974.

Imai, Y., Matshushima, Y., Sugimura, T., & M., T. (1991) *Nucleic Acids Res. 19*, 2785.

Jackson, R. J., & Kaminski, A. (1995) *RNA 1*, 985−1000.

Jansen-Durr, P., Boshart, M., Lupp, B., Bosserhoff, A., Frank, R. W., & Schutz, G. (1992) *Nucleic Acids Res. 20*, 1243−1249.

Kaminski, A., Hunt, S. L., Patton, J. G., & Jackson, R. J. (1995) *RNA 1*, 924−938.

Kanaar, R., A. L., L., Rudner, D. Z., Wemmer, D. E., & Rio, D. C. (1995) *EMBO J. 14*, 4530−4539.

Kenan, D. J., Query, C. C., & Keene, J. D. (1991) *Trends Biochem. Sci. 16*, 214−220.

Kharrat, A., Macias, M. J., Gibson, T. J., Nilges, M., & Pastore, A. (1995) *EMBO J. 14*, 3572−3584.

Kiledjian, M., & Dreyfuss, G. (1992) *EMBO J. 11*, 2655−2664.

LaCasse, E. C., & Lefebvre, Y. A. (1995) *Nucleic Acids Res. 23*, 1647−1656.

Lee, W.-C., Xue, Z., & Melese, T. (1991) *J. Cell Biol. 113*, 1−12.

Lee, A. L., Kanaar, R., Rio, D. C., & Wemmer, D. E. (1994) *Biochemistry 33*, 13775−13786.

Lin, C.-H., & Patton, J. G. (1995) *RNA 1*, 234−245.

Lohman, T. M., & Bujalowski, W. (1990) in *The Biology of Nonspecific DNA-Protein Interactions* (Revzin, A., Ed.) CRC Press, Boca Raton, FL.

Lohman, T. M., Bujalowski, W., & Overman, L. B. (1988) *Trends Biochem. Sci. 13*, 250−255.

Lohman, T. M., & Overman, L. B. (1985) *J. Biol. Chem. 260*, 3594−3603.

Lu, J., & Hall, K. B. (1995) *J. Mol. Biol. 247*, 739−752.

Lutz-Freyermuth, C., Query, C. C., & Keene, J. D. (1990) *Proc. Natl. Acad. Sci. 87*, 6393−6397.

Manavalan, P., & Johnson, W. C. (1987) *Anal. Biochem. 167*, 76−85.

Manley, J. L., & Tacke, R. (1996) *Genes Dev. 10*, 1569−1579.

Matera, A. G., Frey, M. R., Margelot, K., & Wolin, S. L. (1995) *J. Cell Biol. 129*, 1181−1193.

Mayeda, A., Munroe, S. H., Caceres, J. F., & Krainer, A. R. (1994) *EMBO J. 13*, 5483−5495.

McAfee, J. G., Soltaninassab, S. E., Lindsay, M. E., & LeStourgeon, W. M. (1995) *Biochemistry 35*, 1212−1222.

McAfee, J. G., Milam, L. S., Soltaninassab, S. R., & LeStourgeon, W. M. (1996) *RNA 2*, 1139−1152.

Mullen, M. P., Smith, C. W. J., Patton, J. G., & Nadal-Ginard, B. (1991) *Genes Dev. 5*, 642−655.

Munroe, S. H., & Dong, X. (1992) *Proc. Natl. Acad. Sci. 89*, 895−899.

Musco, G., Stier, G., Joseph, C., Morelli, M. A. C., Nilges, M., Gibson, T. J., & Pastore, A. (1996) *Cell 85*, 237−245.

Nagai, K., Oubridge, C., Jessen, T., Li, J., & Evans, P. R. (1990) *Nature 348*, 515−520.

Nagai, K., Oubridge, C., Ito, N., Avis, J., & Evans, P. (1995) *Trends Biochem. Sci. 20*, 233−241.

Nietfeld, W., Mentzel, H., & Pieler, T. (1990) *EMBO J. 9*, 3699−3705.

Oubridge, C., Ito, N., Evans, P. R., Teo, C.-H., & Nagai, K. (1994) *Nature 372*, 432−438.

Patton, J. G., Mayer, S. A., Tempst, P., & Nadal-Ginard, B. (1991) *Genes Dev. 5*, 1237−1251.

Patton, J. G., Porro, E. B., Galceran, J., Tempst, P., & Nadal-Ginard, B. (1993) *Genes Dev. 7*, 393−406.

Pérez, I., Lin, C.-H., McAfee, J. G., & Patton, J. G. (1997) *RNA 3*, 764−778.

Piñol-Roma, S., Swanson, M. S., Gall, J. G., & Dreyfuss, G. (1989) *J. Cell Biol. 109*, 2575−2587.

Romac, J. M.-J., Graff, D. H., & Keene, J. D. (1994) *Mol. Cell. Biol. 14*, 4662−4670.

Sachs, A. B., Davis, R. W., & Kornberg, R. D. (1987) *Mol. Cell. Biol. 7*, 3268−3276.

Scherly, D., Boelens, W., Nathan, N. A., van Venrooij, W. J., & Mattaj, I. W. (1990a) *Nature 345*, 502−506.

Scherly, D., Dathan, N. A., Boelens, W., van Venrooij, W. J., & Mattaj, I. W. (1990b) *EMBO J. 9*, 3675−3681.

Shamoo, Y., Abdul-Manan, N., & Williams, K. R. (1995) *Nucleic Acids Res. 23*, 725−728.

Singh, R., Valcárcel, J., & Green, M. R. (1995) *Science 268*, 1173−1176.

Wang, J., & Bell, L. R. (1994) *Genes Dev. 8*, 2072−2085.

Williams, K. R., Murphy, J. B., & Chase, J. W. (1984) *J. Biol. Chem. 259*, 11804−11811.

Wittekind, M., Görlach, M., Friedrichs, M., Dreyfuss, G., & Mueller, L. (1992) *Biochemistry 31*, 6254−6265.

Zamore, P. D., Patton, J. G., & Green, M. R. (1992) *Nature 355*, 609−614.

BI9711745